Engineering Fracture Mechanics Vol. 42, No. 4, pp. 617–627, 1992
Printed in Great Britain.

0013-7944/92 \$5.00 + 0.00

STRAIN LOCALIZATION IN AXIALLY-SYMMETRIC COMPRESSION OF BRITTLE-COHESIVE MATERIALS

DAVIDE BIGONI
Istituto di Scienza delle Costruzioni, Facoltà di Ingeneria, Università di Bologna, viale Risorgimento 2, 40136 Bologna, Italy

Abstract—It is shown that strain localization occurring in the positive hardening regime of axially-symmetric compression stress states, may be modeled through a proper choice of the yield function and flow-mode, in the context of the infinitesimal rate-independent non-associative elastoplasticity. In this way, it becomes possible to interpret the results of the uniaxial compression tests carried out on concrete and fiber-reinforced concrete specimens.

1. INTRODUCTION

THE STRAIN localization analysis of an elastoplastic continuum was introduced by Rudnicki and Rice [1], Rice [2] and Vardoulakis [3] as a model to predict the onset of localization of microdamage in metallic as well as in rock-like materials, for which the localization of deformation represents a tool for detecting the onset of brittle fracture.

Recently, the strain localization concept was proposed as a possible key for understanding the behavior of brittle-cohesive materials (concrete, rock) under multi(uni)-axial compression [4–7]. Such materials, in fact, exhibit a softening behavior which is very sensitive to the testing conditions (boundary conditions of the specimen), along with a pronounced size effect, both effects being explained on the basis of strain localization phenomena. In this frame of research, the series of uniaxial compression tests, performed at the Laboratoire Central des Pontes et Chaussees (LCPC) of Paris on samples of concrete and fiber-reinforced concrete [8–11], can be located. The tests have shown a number of important and unknown features of localization of microcracking in concrete. In particular:

(1) localization of deformation always precedes the peak of the uniaxial stress–strain curve, i.e. localization occurs in the hardening regime;
(2) rotation of the loading platens begins only *after* the onset of localization (i.e. "tilting" is absent before localization).

Moreover, the localization bands have been shown to form angles with respect to the compression axis, which are always less than (approximately) 45° and are always accompanied by volumetric dilatancy.

Result (1) was precognized and indirectly verified by van Mier [12] and may now be considered as generally accepted [7]. Moreover, a qualitatively similar result was obtained in sand specimens [13, 14], using the biaxial test [15].

Result (2) allows one to conclude that localization of deformation in concrete cannot be strongly affected by unstabilizing effects due to geometrical changes (e.g. those investigated in [1] and [16]).

From the point of view of constitutive modeling, using the Drucker–Prager non-associative model of Rudnicki and Rice [1], strain localization in axially-symmetric compression becomes possible only in the softening regime. The same circumstance is verified even when co-rotational terms are taken into account in the constitutive law [1]. Even in the cases of the multi-response model [17], the thermoelastic–plastic model [18] and the elastoplastic–fracturing model [19], strain localization becomes possible only in the softening regime for axially-symmetric compression. Finally, strain localization is predicted not to occur, in uniaxial compression, for the model proposed by Ortiz [20, 21]. These results induce a skepticism regarding the possibility of modeling the strain localization occurring during the hardening regime of axially-symmetric compression and therefore of reproducing the mentioned experimental results.

Despite the above skepticism, this paper shows that the strain localization during the hardening regime in axially-symmetric compression can occur if a yield surface and a plastic potential of an appropriate shape are adopted, in the context of a single, smooth yield and plastic-potential surface, non-associative elastoplasticity. From the point of view of constitutive modeling of concrete, however, the available experimental work does not allow for the development of a complete model for strain localization of concrete under complex stress conditions. Therefore, this paper can be regarded as an initial contribution towards the definition of a model capable of reproducing localization of damage in brittle-cohesive materials (concrete and fiber-reinforced concrete).

2. MATERIAL MODEL

The elastoplastic behavior is characterized here by an incremental stress–strain relationship, relating the derivative of the Cauchy stress $\mathbf{T}$ to the velocity of deformation $\mathbf{D}$

$$\dot{\mathbf{T}} = \mathbb{D}[\mathbf{D}], \tag{1}$$

where the operator $\mathbb{D}$ defines a two-tensorial zone constitutive equation [22]. In fact, $\mathbb{D}$ is piecewise linear and different in the case of plastic loading or elastic unloading (or neutral loading)

$$\mathbf{N}\cdot\mathbb{E}[\mathbf{D}] \geqslant 0 \Rightarrow \mathbb{D} = \mathbb{E} - \frac{\mathbb{E}[\mathbf{M}] \otimes \mathbb{E}[\mathbf{N}]}{h + h_0} \tag{2}$$

$$\mathbf{N}\cdot\mathbb{E}[\mathbf{D}] \leqslant 0 \Rightarrow \mathbb{D} = \mathbb{E}, \tag{3}$$

where $\mathbb{E}$ is the elastic fourth order tensor, $\mathbf{N}$ is the (unit norm) gradient of the yield function f and $\mathbf{M}$ is the (unit norm) tensor that specifies the direction of the plastic component $\mathbf{D}^p$ of the velocity of deformation

$$\mathbf{N} = \frac{\nabla f}{\sqrt{(tr(\nabla f^2))}} \tag{4a}$$

$$\mathbf{M} = \frac{\mathbf{D}^p}{\sqrt{(\mathbf{D}^p\cdot\mathbf{D}^p)}}. \tag{4b}$$

The scalars h (hardening modulus) and h_0 in eq. (2) are defined as

$$h = -\frac{1}{\sqrt{(tr(\nabla f^2))}}\left[\sum_{i=1}^{n}\frac{\partial f}{\partial k_i}\dot{k}_i + \sum_{i=1}^{m}\frac{\partial f}{\partial \mathbf{K}_i}\cdot\dot{\mathbf{K}}_i\right], \quad h_0 = \mathbf{N}\cdot\mathbb{E}[\mathbf{M}], \tag{5}$$

in which k_i and $\mathbf{K}_i$ denote the collection of the state variables (mixed kinematic–isotropic hardening). Positive values of h correspond to positive hardening, whereas a negative value of h denotes softening behavior ($h = 0$ identifies the perfect-plasticity). Note that eqs (1)–(5) are related to each other via the Prager consistency condition [23].

Here the elastic response is restricted to be represented by a linear isotropic mapping Sym→Sym

$$\mathbb{E} = \lambda\mathbf{I}\otimes\mathbf{I} + 2\mu\mathbb{I}, \tag{6}$$

where λ and μ are the Lamé constants and $\mathbf{I}$ and $\mathbb{I}$ are the second and fourth order identity tensors, respectively.

3. THE LOCALIZATION OF DEFORMATION IN AXIALLY-SYMMETRIC COMPRESSION

The localization of deformation into planar bands is attained when the constitutive equation suffers a loss of ellipticity [2], i.e. when

$$(\exists\mathbf{n}, \mathbf{g} \neq \mathbf{0}) \quad \mathbb{D}[\mathbf{g}\otimes\mathbf{n}]\mathbf{n} = \mathbf{0}, \tag{7}$$

where $\mathbf{n}$ is the unit vector normal to the band and vector $\mathbf{g}$ is parallel to the velocity inside the band ($\mathbf{n}$ and $\mathbf{g}$ so defining the mode of localization). It is a well-known result [24] that the first possible localization threshold is attained in a loading program, when a loss of ellipticity occurs in the comparison solid corresponding to the loading branch of the relationship (1). In other words, the first localization threshold is determined by the condition (7) where the operator $\mathbb{D}$ is identified with the tensor (2). In this case, condition (7) may be given in terms of a critical value of the hardening modulus [2]

$$\mathscr{h}_{cr} = \max_{\mathbf{n}} \left\{ 2G\left[2\mathbf{n}\otimes\mathbf{n}\cdot\mathbf{MN} - (\mathbf{n}\cdot\mathbf{Mn})(\mathbf{n}\cdot\mathbf{Nn}) - \mathbf{M}\cdot\mathbf{N} - \frac{\nu}{1-\nu}(\mathbf{n}\cdot\mathbf{Mn} - tr\ \mathbf{M})(\mathbf{n}\cdot\mathbf{Nn} - tr\ \mathbf{N}) \right]\right\}, \tag{8}$$

subject to the condition $\mathbf{n}\cdot\mathbf{n} = 1$, where ν is the Poisson ratio and G the elastic shear modulus. For the unit vector $\mathbf{n}$ that maximizes eq. (8), the corresponding vector $\mathbf{g}$ is given by [2]

$$\mathbf{g}(\mathbf{n}) = 2\mathbf{Mn} - \frac{1}{1-\nu}(\mathbf{n}\cdot\mathbf{Mn})\mathbf{n} + \frac{\nu}{1-\nu}(tr\ \mathbf{M})\mathbf{n}. \tag{9}$$

At a generic point of an elastoplastic body, during a loading history, localization is excluded until the actual hardening modulus remains greater than the critical one. The first possibility of localization is attained when $\mathscr{h} = \mathscr{h}_{cr}$. In [25], it is shown that a general explicit solution to condition (8) can be obtained when tensors $\mathbf{N}$ and $\mathbf{M}$ are coaxials (i.e. when $\mathbf{M}$ and $\mathbf{N}$ commute: $\mathbf{MN} = \mathbf{NM}$). In particular, $\mathbf{M}$ and $\mathbf{N}$ are necessarily coaxials in the case of isotropic hardening or in the case when $\mathbf{M}$ is defined as an isotropic function of $\mathbf{N}$ (e.g. in the case of deviatoric normality [26]). In any case, for an axially-symmetric stress condition, starting from a virgin state, tensors $\mathbf{M}$ and $\mathbf{N}$ remain coaxial by adopting Prager's or Zielger's kinematic hardening rules.

In the case of axially-symmetric stress states, tensors $\mathbf{D}$, $\mathbf{N}$, $\mathbf{M}$ and $\mathbf{K}_i$ are axially-symmetric before strain localization. Therefore, the direction of the normal to the band is individuated from (8) with respect to the symmetry axis only. Without loss of generality, an orthogonal reference system may be chosen having the axis 3 coincident with the symmetry axis and axis 1 defining, together with axis 3, the plane in which the normal to the band $\mathbf{n}$ lies. This reference system is a principal reference system for tensors $\mathbf{M}$ and $\mathbf{N}$ which have the following spectral representation:

$$\mathbf{M} = \mathbf{e}_1\otimes\mathbf{e}_1 M_1 + \mathbf{e}_2\otimes\mathbf{e}_2 M_2 + \mathbf{e}_3\otimes\mathbf{e}_3 M_3 \tag{10}$$

$$\mathbf{N} = \mathbf{e}_1\otimes\mathbf{e}_1 N_1 + \mathbf{e}_2\otimes\mathbf{e}_2 N_2 + \mathbf{e}_3\otimes\mathbf{e}_3 N_3, \tag{11}$$

where $M_1 = M_2 \neq M_3$ and $N_1 = N_2 \neq N_3$ are the eigenvalues and $\mathbf{e}_1$, $\mathbf{e}_2$, and $\mathbf{e}_3$ the eigenvectors of tensors $\mathbf{M}$ and $\mathbf{N}$. In the chosen reference system, the components of the normal to the band satisfy the conditions

$$n_1^2 = 1 - n_3^2, \quad n_2 = 0. \tag{12}$$

Using eqs (10)–(12), the condition (8) may be written (in the reference system $\mathbf{e}_1, \mathbf{e}_2, \mathbf{e}_3$, i.e. in the case of axially symmetric compression) as

$$\mathscr{h}_{cr} = \max_{n_3^2} \mathscr{h}(n_3^2), \quad 0 \leqslant n_3^2 \leqslant 1, \tag{13}$$

where

$$\begin{aligned}\mathscr{h}(n_3^2) = 2G\Big\{ n_3^2 \Big\{ & 2(M_3N_3 - M_1N_1) - \frac{1}{1-\nu}[(M_3 - M_1)N_1 + (N_3 - N_1)M_1] \\ & + \frac{\nu}{1-\nu}[tr\ \mathbf{N}(M_3 - M_1) + tr\ \mathbf{M}(N_3 - N_1)]\Big\} - n_3^4\left[\frac{1}{1-\nu}(M_3 - M_1)(N_3 - N_1)\right] \\ & - M_3N_3 - M_1N_1 - \frac{\nu}{1-\nu}(N_3 + N_1)(M_3 + M_1)\Big\}.\end{aligned} \tag{14}$$

Hence, the constrained maximization problem (13) may be easily solved, yielding a different result of either

$$(M_3 - M_1)(N_3 - N_1) \geqslant 0 \tag{15}$$

or

$$(M_3 - M_1)(N_3 - N_1) < 0. \tag{16}$$

In the case when eq. (15) holds, the maximum of eq. (14) is attained in correspondence of

$$n_3^2 = 1 - \langle 1 - \langle \chi \rangle \rangle, \tag{17}$$

where the operator $\langle\,\rangle$ represents the McAulay brackets [i.e. the operator $\mathbb{R} \to \mathbb{R}^+ + \{0\}$, $\forall x \in \mathbb{R}$, $\langle x \rangle = (x + |x|)/2$] and χ is given by

$$\chi = (1 - \nu)\frac{M_3 N_3 - M_1 N_1}{(M_3 - M_1)(N_3 - N_1)} - \frac{N_1}{2(N_3 - N_1)} - \frac{M_1}{2(M_3 - M_1)} + \frac{\nu(N_3 + 2N_1)}{2(N_3 - N_1)} + \frac{\nu(M_3 + 2M_1)}{2(M_3 - M_1)}. \tag{18}$$

Note that, when eq. (15) holds and $0 < \chi < 1$, the value of n_3^2 given by eq. (17) corresponds to an analytical maximum of eq. (14).

In the case when eq. (16) holds, the maximum of eq. (14) is obtained in correspondence of $n_3^2 = 0$ or $n_3^2 = 1$.

In the given reference system, for axially-symmetric compression, the stress state is characterized by the principal components of the stress tensor $\mathbf{T}$

$$T_3 < T_1 = T_2 \leqslant 0. \tag{19}$$

The following *constitutive assumptions* regarding the behavior of material in axially-symmetric compression are now introduced:

$$M_3 < 0 \tag{20}$$

$$\mathbf{M} \cdot \mathbf{N} > 0 \tag{21}$$

$$tr\,\mathbf{M} \geqslant 0. \tag{22}$$

From eq. (4b) it is seen that condition (20) has an obvious physical meaning, whereas condition (21), which excludes a plastic flow directed inside the yield surface, is generally accepted (see e.g. [27]). Finally, condition (22) requires that the volumetric component of the plastic flow be positive and is accepted here because of the experimental observation that localization of deformation in brittle-cohesive materials (e.g. concrete) is accompanied by dilatancy. Also note that the minimum requirement that the yield function be a star-shaped surface centered in the point $\mathbf{T} = \mathbf{0}$ [28], implies $-1 \leqslant N_3 \leqslant 0$.

When conditions (20)–(22) are assumed, condition (15) holds true and the critical modulus for localization in the case of the axially-symmetric compression [i.e. the solution of eq. (13)] is obtained by substituting eq. (17) into eq. (14).

3.1. *Associative flow rule*

In the case of the associative flow rule, $\mathbf{M} = \mathbf{N}$, and eq. (18) reduces to

$$\chi = \frac{N_3 + \nu N_1}{N_3 - N_1}. \tag{23}$$

The critical hardening modulus for localization in the case of the axially-symmetric compression results to be given [through substitution of eq. (23) into eq. (14)] by

$$h_{cr} = -2G(1 + \nu)N_1^2 - \frac{2G}{1 - \nu}\left[\frac{\langle -\chi \rangle}{-\chi}(N_3 + \nu N_1)^2 + \frac{\langle \chi - 1 \rangle}{\chi - 1}(N_1 + \nu N_1)^2\right]. \tag{24}$$

From eq. (24) it is seen that localization cannot occur for associative plasticity in the hardening regime (this is a well-known result [2]). Moreover, in the compression test, the localization can occur at the peak of the stress–strain curve when $h_{cr} = 0$. This condition can be attained if $N_1 = 0$ and $\chi \in [0, 1]$ [see eq. (24)], corresponding to $n_3 = 1$, i.e. to a band that is orthogonal to the direction of compression.

It is therefore concluded that the behavior of concrete at localization in the compression test cannot be interpreted via associative plasticity. In fact, localization is observed to occur just before the peak and the band is far from being orthogonal to the compression axis.

3.2. *Non-associative flow rule*

Having assumed that $\mathbf{M}\cdot\mathbf{M} = \mathbf{N}\cdot\mathbf{N} = 1$, tensors $\mathbf{M}$ and $\mathbf{N}$ are represented in the Haigh–Westergaard stress space as unit vectors. Moreover, the principal components M_3, N_3 must be negative and therefore, if components $M_1 = M_2$ and $N_1 = N_2$ are assigned, M_3 and N_3 are known. Using eqs (17), (16) and (14) it becomes possible, for a given value of v, to evaluate ℓ_{cr}/G as a function of M_3 and N_1. For instance, if $tr\ \mathbf{M} = 0$ and $N_1 = N_2 = 0$ (i.e. $N_3 = -1$) are assumed, $n_3^2 = 5/6$ and $\ell_{cr}/G \cong 0.0340$ are found for $v = 0$; in this case, ℓ_{cr} always results to be positive for $v \geqslant 0$.

Thus, in the case of non-associative plasticity, strain localization during positive hardening is possible for axially-symmetric compression, for appropriate directions of yield surface gradient and plastic flow.

In Fig. 1 the values of ℓ_{cr}/G are reported as functions of N_1, for $v = 0$ and for different values of M_3 ($-\sqrt{(2/3)}$, -0.60, -0.45, -0.30). In Fig. 2, as functions of the same parameters, the values of the angle ϑ between the normal to the band and the axis of compression are reported. Figures 3 and 4 show the same type of graphs as in Figs 1 and 2, for $v = 0.15$. Finally, in Figs 5 and 6 (for $M_3 = -\sqrt{(2/3)}$) and 7 and 8 (for $M_3 = -0.3$) the values of ℓ_{cr}/G and ϑ are reported, as functions of N_1, for different values of v (0, 0.15, 0.30, 0.45). The extreme values of $M_3 = -\sqrt{(2/3)}$ and $M_3 = -0.30$ have been selected since $M_3 = -\sqrt{(2/3)}$ corresponds to isochoric plastic flow ($tr\ \mathbf{M} = 0$) and $M_3 = -0.30$ corresponds to a very pronounced dilatancy for rock-like materials (see e.g. [1]).

From the localization condition (13)–(17) and the results reported in the quoted figures, the following observations can be drawn.

—The critical hardening modulus for localization is *positive* in the uniaxial compression state for values of N_1 less than (about) 0.30, corresponding to values of N_3 less than (about) -0.90. A unit vector normal to the hydrostatic axis and lying on the triaxial plane, has a component along the axis T_3 equal to $-\sqrt{(2/3)} \cong -0.82 > -0.90$; thus a yield surface having $M_3 \leqslant -0.90$ must, if convex, intersect the hydrostatic axis.

—The critical hardening modulus, when positive, increases with v and M_3 (i.e. ℓ_{cr} increases when the "degree of non-associativity" increases).

—Bands orthogonal or parallel to the direction of compression are, in principle, possible. In fact, the first case was encountered, for instance, when the associative flow rule was considered. The latter case occurs, for example, when $N_1 > 0.60$ for $v = 0.45$ (see Fig. 8). The case of bands parallel to the direction of compression seems, however, to involve "unusual" constitutive parameters. For example, bands parallel to the direction of compression can develop in the case of the Mohr–Coulomb yield criterion with non-associative flow rule satisfying eqs (20)–(22). In particular, this possibility arises when null cohesion and the shearing resistance angle equal to 90° are assumed and when the plastic flow satisfies

$$(1 - v)M_3 + 2vM_1 \geqslant 0. \tag{25}$$

Condition (25) has been obtained keeping in mind that, with the assumed material parameters, the yield surface gradient satisfies $N_3 = 0$, and imposing the condition $\chi \leqslant 0$ into eq. (18).

—The critical hardening modulus increases when N_1 decreases and is negative. However, the angle ϑ decreases (the band tends to become orthogonal to the direction of compression) when N_1 decreases.

In order to simulate the behavior of brittle-cohesive materials such as concrete, an elastoplastic model of the type described in Section 2 must possess the following general requisites *at localization of deformation.*†

—The yield surface, if convex, must intersect the hydrostatic axis, i.e. inelastic strain must initiate (at a curtain level) for isotropic compression. This feature of the yield function is in agreement with experimental observations [29] and is found in many elastoplastic models (e.g. [30–32]).

†It is important to observe that the form of the yield surface at localization could result from a complex hardening evolution. Thus, the shape of the yield function at localization could be very different from the shape of the same function for the virgin material.

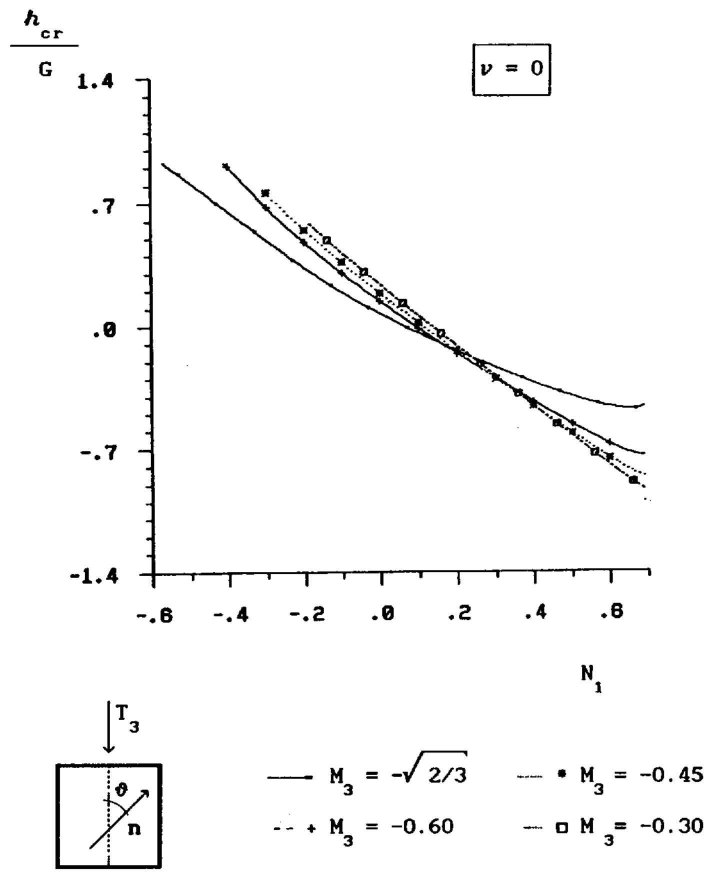

Fig. 1. Critical hardening modulus for localization vs N_1 as function of the "degree of non-associativity" M_3.

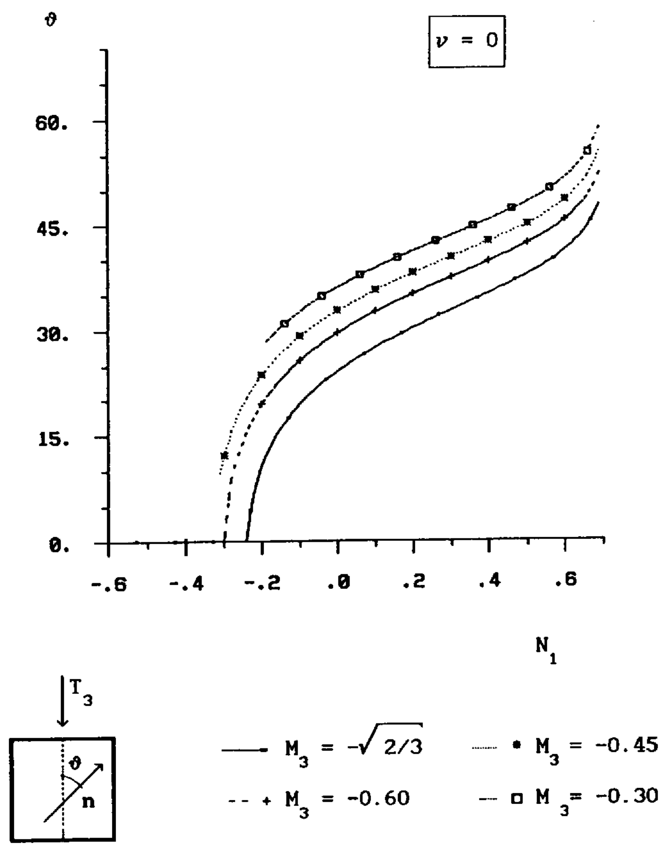

Fig. 2. Angle (in degrees) of inclination of the normal to the localization band with respect to the compression axis vs N_1.

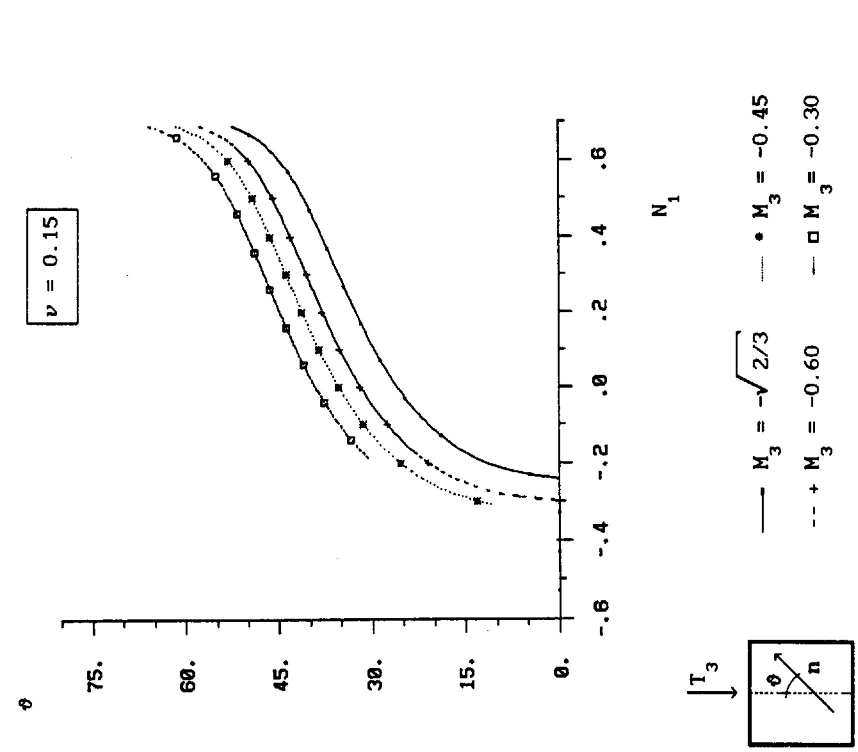

Fig. 4. Angle (in degrees) of inclination of the normal to the localization band with respect to the compression axis vs N_1.

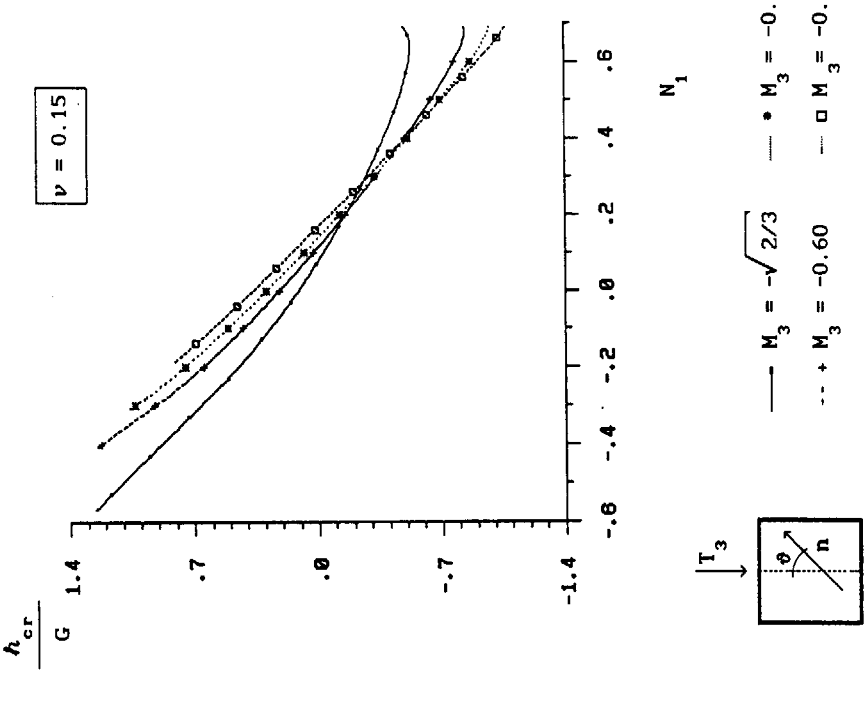

Fig. 3. Critical hardening modulus for localization vs N_1 as function of the "degree of non-associativity" M_3.

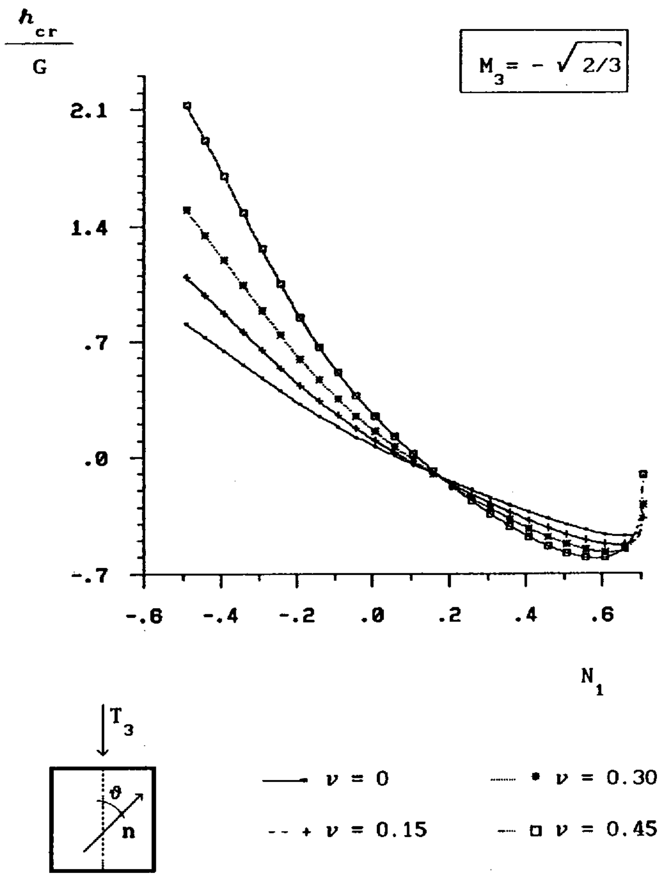

Fig. 5. Critical hardening modulus for localization vs N_1 as function of the Poisson ratio ν.

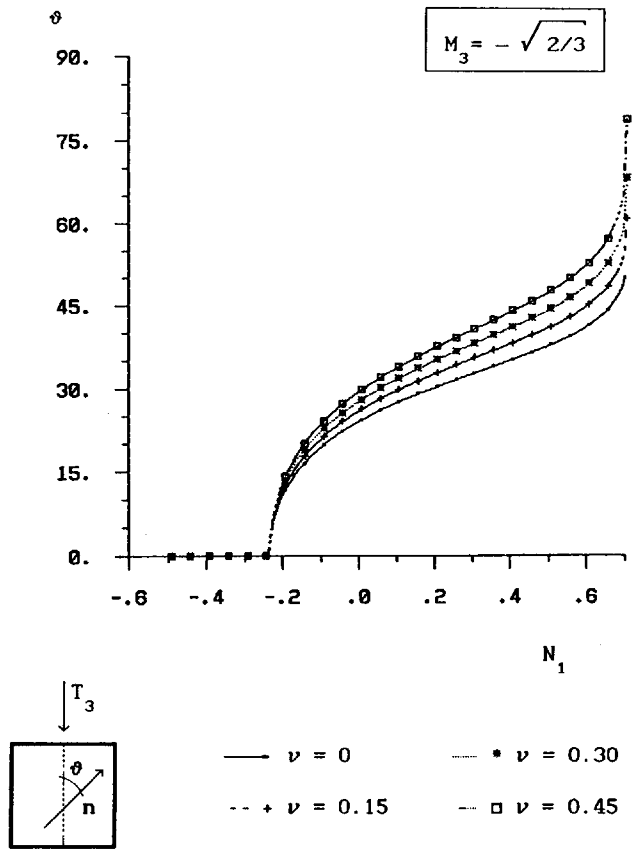

Fig. 6. Angle (in degrees) of inclination of the normal to the localization band with respect to the compression axis vs N_1.

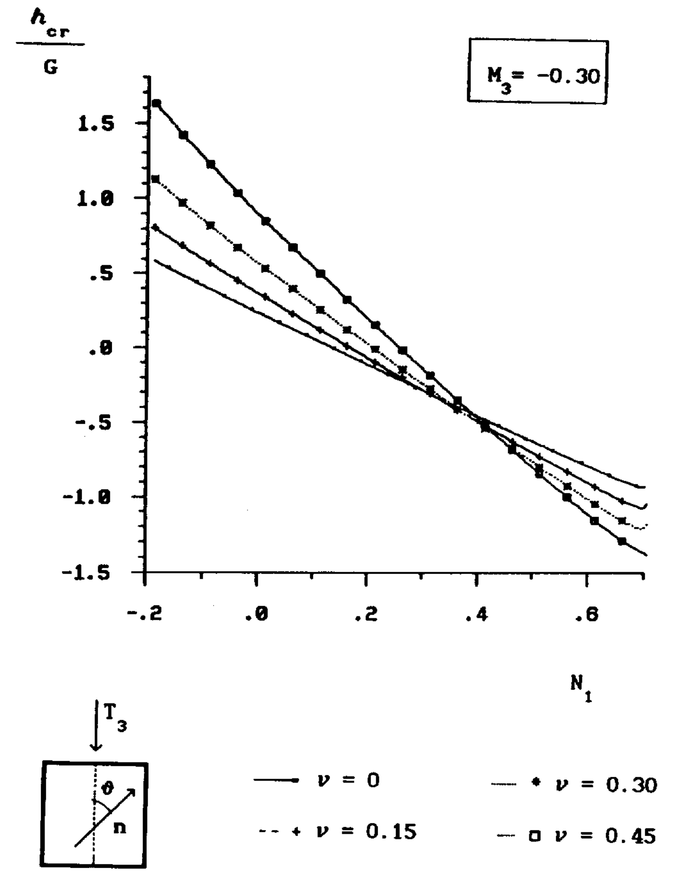

Fig. 7. Critical hardening modulus for localization vs N_1 as function of the Poisson ratio ν.

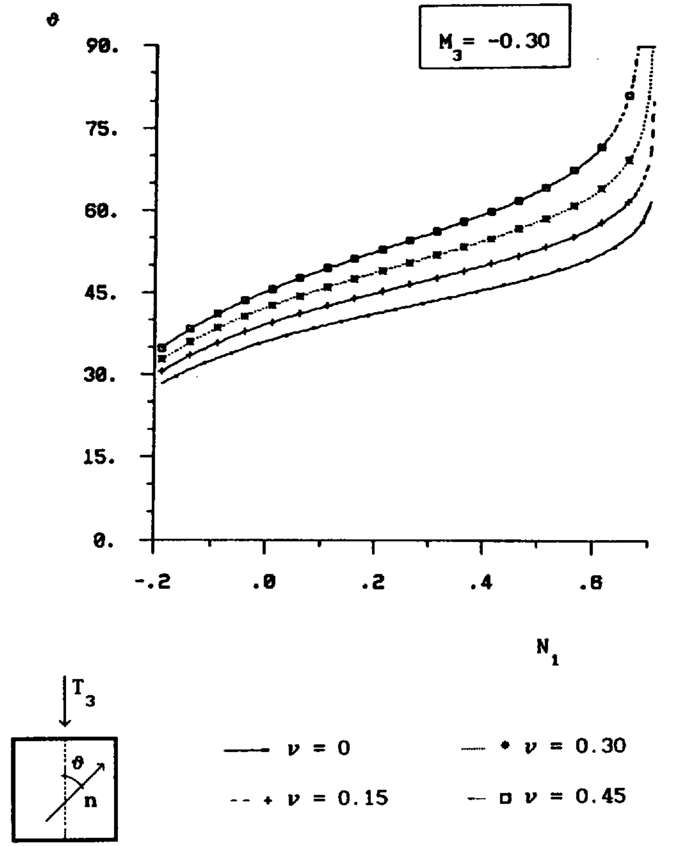

Fig. 8. Angle (in degrees) of inclination of the normal to the localization band with respect to the compression axis vs N_1.

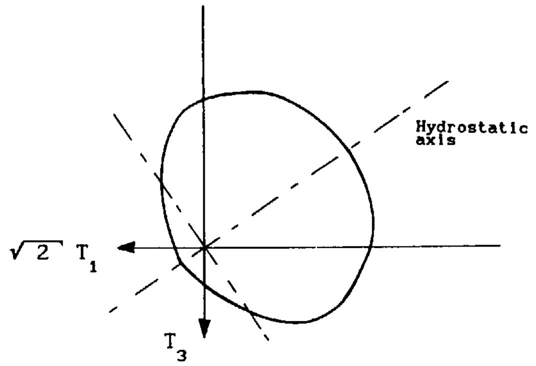

Fig. 9. Qualitative shape of the intersection of the yield function with the triaxial plane.

—The gradient of the yield function at the point of intersection with the compression axis (T_3), must lie very near to the axis T_3 (i.e. $N_3 < -0.90$). At least from a qualitative examination, this condition is not found in the models in [30–32].

—The experimental observation that, for concrete and fiber-reinforced concrete, bands always make angles less than 45° with respect to the direction of compression excludes negative values of N_1. In fact, for N_1 negative, the angles ϑ are always less than 45° (see Figs 2, 4, 6 and 8).

Finally it can be concluded that the yield function, *at localization*, must possess, qualitatively, an intersection as shown in Fig. 9 with the plane containing the hydrostatic axis and the compression axis (triaxial plane). Note that, for the sake of simplicity, symmetry about the hydrostatic axis has been assumed. A yield surface having the shape shown in Fig. 9, together with a non-associative flow rule (excluding plastic volumetric contraction), can predict localization during axially-symmetric compression in the positive hardening regime.

4. CONCLUSIONS

Experiments performed at the Laboratoire Central des Ponts et Chaussees (LCPC) of Paris on concrete and fiber-reinforced concrete samples have shown, among many other relevant unknown behaviors, that localization of deformation during uniaxial compression occurs in the positive hardening regime [8–11]. Moreover, localization occurs in absence of relevant unstabilizing effects of geometric nature and is accompanied by volumetric dilatancy. On the other hand, strain localization cannot precede the peak of the stress–strain curve in axially-symmetric compression, in the case of models analyzed in [1, 17–21].

In this paper it has been shown that, for a proper choice of the shape of the yield surface and the direction of the plastic flow, it is possible to model strain localization during the hardening regime for axially-symmetric compression stress states. In particular, strain localization can occur in the positive hardening regime if the yield surface intersects the hydrostatic axis. It is also shown that this possibility of modeling localization is excluded by adopting the associative flow rule. Finally, in the context of modeling the behavior of brittle-cohesive materials, the experimental results presently available are not sufficient to develop a complete model for the localization of deformation for stress states different from that of uniaxial compression. In particular, an experimental investigation on strain localization in triaxial loading conditions is needed and therefore the presented model is an initial contribution in the direction of modeling strain localization in concrete.

Acknowledgments—The author would like to thank Dr. P. Acker, Dr. J. M. Torrenti and Dr. E. H. Benaija of the Laboratoire Central des Ponts et Chaussees (Paris) for their kind hospitality and for having discussed and provided the author with the experimental results on which this paper is based. A grateful acknowledgment is also due to the Italian Ministry of University and Scientific and Technological Research.

REFERENCES

[1] J. W. Rudnicki and J. R. Rice, Conditions for the localization of deformations in pressure-sensitive dilatant materials. *J. Mech. Phys. Solids* **23,** 371–394 (1975).

[2] J. R. Rice, The localization of plastic deformation, in *Theoretical and Applied Mechanics* (Edited by W. T. Koiter), pp. 207–220. North-Holland, Amsterdam (1976).

[3] I. Vardoulakis, Equilibrium theory of shear bands in plastic bodies. *Mech. Res. Commun.* **3**(3), 209–214 (1976).

[4] P. Habib, Multiaxial testing of concrete, final report—introduction. *Mater. Structures* **24,** 38–41 (1991).

[5] M. Ortiz, Extraction of constitutive data from specimens undergoing strain localization. *J. Engng Mech., ASCE* **115,** 1748–1760 (1989).

[6] J. M. Torrenti, Some remarks upon concrete softening. *Materiaux Constructions* **19**(113), 391–393 (1986).

[7] J. G. M. van Mier and R. A. Vonk, Fracture of concrete under multaxial stress—recent developments. *Mater. Structures* **21,** 61–65 (1991).

[8] E. H. Benaija, Application of stereophotogrammetry to concrete: the case of uniaxial compression. Ph.D. Thesis, Ecole National des Ponts et Chaussees, Paris (1991) [in French].

[9] J. M. Torrenti and E. H. Benaija, Stereophotogrammetry: a new way to study strain localization in concrete under compression. *9th International Conference on Experimental Mechanics*, Lyngby, Copenhagen (1990).

[10] J. M. Torrenti, J. Desrues, P. Acker and C. Boulay, Application of stereophotogrammetry to the strain localization in concrete compression, in *Cracking and Damage* (Edited by J. Mazars and Z. P. Bazant), pp. 30–41. Elsevier, London (1989).

[11] J. M. Torrenti, J. Desrues and E. H. Benaija, The application of stereophotogrammetry to strain localization in concrete. 1989 *Spring Conference on Experimental Mechanics*, Cambridge, MA (1989).

[12] J. G. M. van Mier, Strain-softening of concrete under multiaxial loading conditions. Ph.D. Thesis, De Technische Hogeschool Eindhoven (1984).

[13] I. Vardoulakis and B. Graf, Calibration of constitutive models for granular materials using data from biaxial experiments. *Geotechnique* **35,** 229–317 (1985).

[14] J. Desrues, Shear band initiation in granular materials: experimentation and theory, in *Geomaterials: Constitutive Equations and Modelling* (Edited by F. Darve), pp. 283–310. Elsevier, Amsterdam (1990).

[15] I. Vardoulakis, Theoretical and experimental bounds for shear-band bifurcation strain in biaxial tests on dry sand. *Res. Mechanica* **23,** 239–259 (1988).

[16] I. Vardoulakis, M. Goldscheider and G. Gudehus, Formation of shear bands in sand bodies as a bifurcation problem. *Int. J. numer. analyt. Meth. Geomech.* **2,** 99–128 (1978).

[17] Y. Ichikawa, T. Ito and Z. Mróz, A strain localization condition applying multi-response theory. *Ing.-Arch.* **60,** 542–552 (1990).

[18] M. Duszek and P. Perzyna, The localization of plastic deformation in thermöplastic solids. *Int. J. Solids Structures* **24,** 1419–1443 (1991).

[19] D. Bigoni and T. Hueckel, Uniqueness and localization. Part II—coupled elastoplasticity. *Int. J. Solids Structures* **28,** 215–224 (1991).

[20] M. Oritz, A constitutive theory for the inelastic behavior of concrete. *Mech. Materials* **4,** 67–93 (1985).

[21] M. Ortiz, An analytical study of the localized failure modes of concrete. *Mech. Materials* **6,** 159–174 (1987).

[22] F. Darve, The expression of rheological laws in incremental form and the main classes on constitutive equations, in *Geomaterials: Constitutive Equations and Modelling* (Edited by F. Darve), pp. 123–147. Elsevier, Amsterdam (1990).

[23] W. Prager, Recent developments in the mathematical theory of plasticity. *J. appl. Phys.* **20**(3), 235–241 (1949).

[24] J. R. Rice and J. W. Rudnicki, A note on some features of the theory of localization of deformation. *Int. J. Solids Structures* **16,** 597–605 (1980).

[25] D. Bigoni and T. Hueckel, Uniqueness and localization. Part I—associative and non-associative elastoplasticity. *Int. J. Solids Structures* **28,** 197–213 (1991).

[26] D. Bigoni and T. Hueckel, A note on strain localization for a class of non-associative plasticity rules. *Ing.-Arch.* **60,** 491–499 (1990).

[27] K. Runesson and Z. Mróz, A note on nonassociated plastic flow rules. *Int. J. Plasticity* **5,** 639–658 (1989).

[28] J. Salençon, *Calcul a la rupture et analyse limite*. Presses de l'Ecole Nationale des Ponts et Chaussees, Paris (1983).

[29] J. M. Torrenti, Comportement multiaxial du beton: aspects experimentaux et modelisation. Ph.D. Thesis, Ecole Nationale des Ponts et Chaussees, Paris (1987).

[30] A. C. T. Chen and W. F. Chen, Constitutive relations for concrete. *J. Engng Mech Div., ASCE* **101**(EM4), 465–481 (1975).

[31] J. G. Merkle, An ellipsoidal yield function for materials that can be both dilate and compact inelastically. *Nucl. Engng Design* **12**(3), 425–451 (1970).

[32] K. H. Roscoe and J. Burland, On generalized stress–strain behavior of wet clay, in *Engineering Plasticity* (Edited by J. Haymann and F. A. A. Leckie), pp. 535–609. Cambridge University Press, Cambridge (1968).

(*Received* 3 *July* 1991)